US 20120004539A1

(19) United States

(12) Patent Application Publication

(10) Pub. No.: US 2012/0004539 A1

(43) Pub. Date: Jan. 5, 2012

Gardi et al.

(54) ULTRASOUND IMAGING SYSTEM AND METHODS OF IMAGING USING THE SAME

(75) Inventors: **Lori Anne Gardi**, London (CA); **Donal B. Downey**, Kamloops (CA); **Aaron Fenster**, London (CA)

(73) Assignee: **Robarts Research Institute**

(21) Appl. No.: **13/233,449**

(22) Filed: **Sep. 15, 2011**

Related U.S. Application Data

(60) Division of application No. 12/706,476, filed on Feb. 16, 2010, now abandoned, which is a continuation of application No. 10/585,984, filed on Jul. 18, 2007, now abandoned, filed as application No. PCT/CA2005/000032 on Jan. 12, 2005.

(60) Provisional application No. 60/535,825, filed on Jan. 13, 2004.

Publication Classification

(51) **Int. Cl.**
A61B 8/00 (2006.01)

(52) **U.S. Cl.** **600/424**

(57) **ABSTRACT**

A method of registering the position of an object moving in a target volume in an ultrasound imaging system includes capturing a first ultrasound image of a target volume. A second ultrasound image of the target volume is then captured after the capturing of the first ultrasound image. The position of the object in the target volume is identified using differences detected between the first and second ultrasound images. In another aspect, a region of interest in the target volume is determined. A segment of an operational scan range of a transducer of the ultrasound imaging system encompassing the region of interest is determined. The transducer is focused on the segment of the operational scan range during image capture.

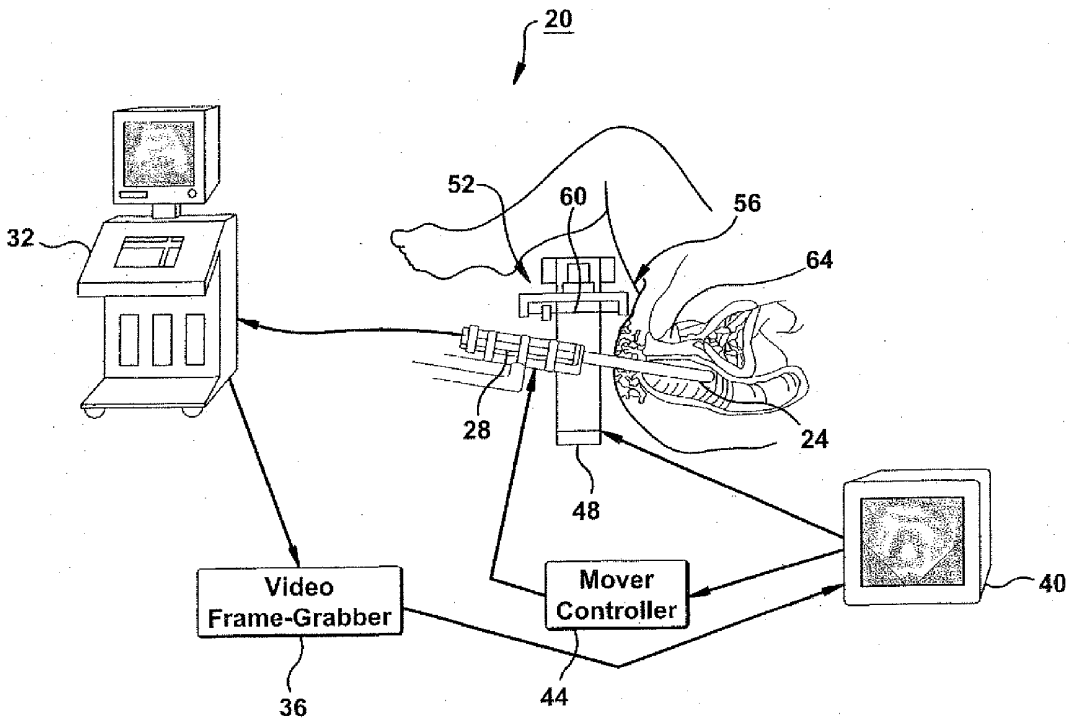

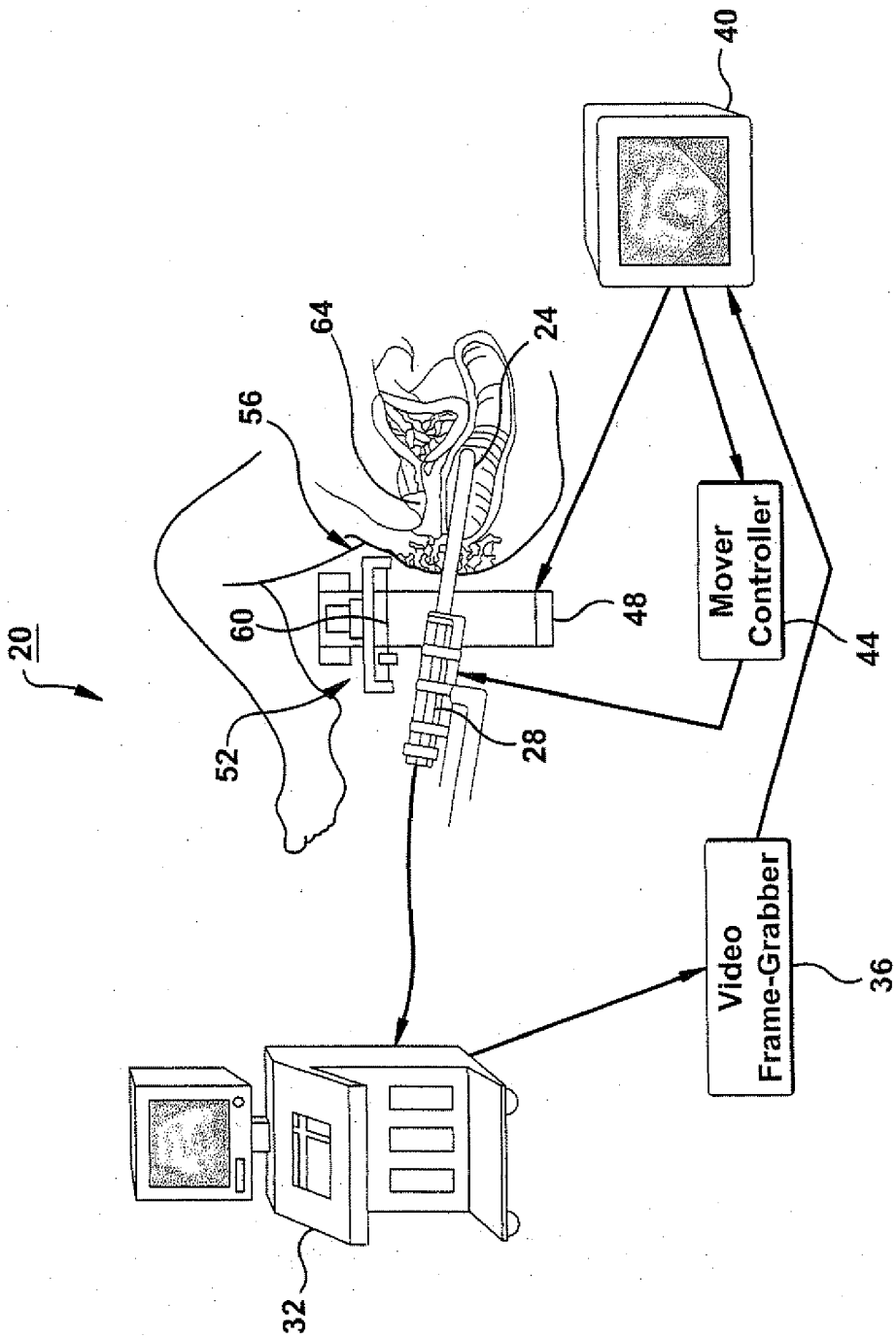
20
40
64
24
56
60
48
52
28
Mover Controller
44
Video Frame-Grabber
36
32

Fig. 1

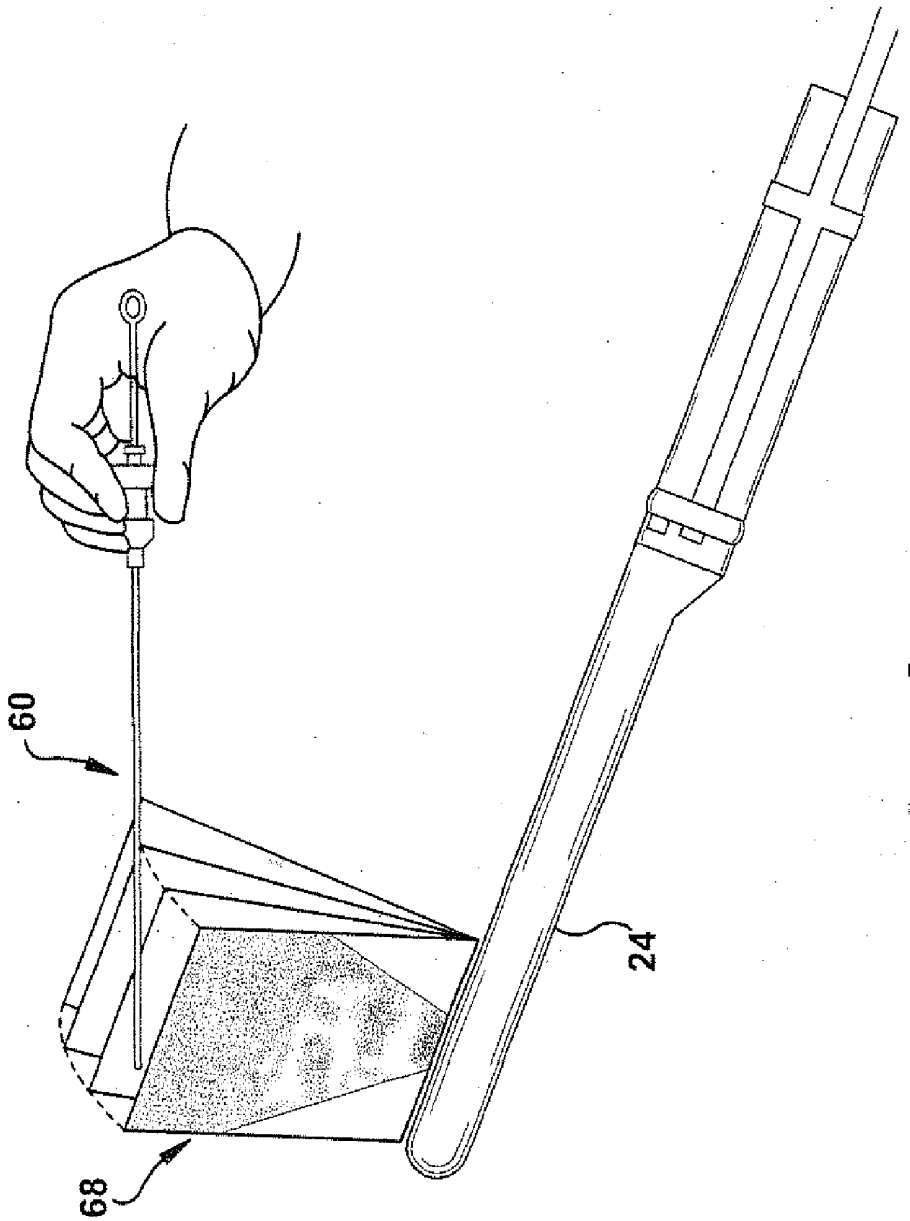

Fig. 2

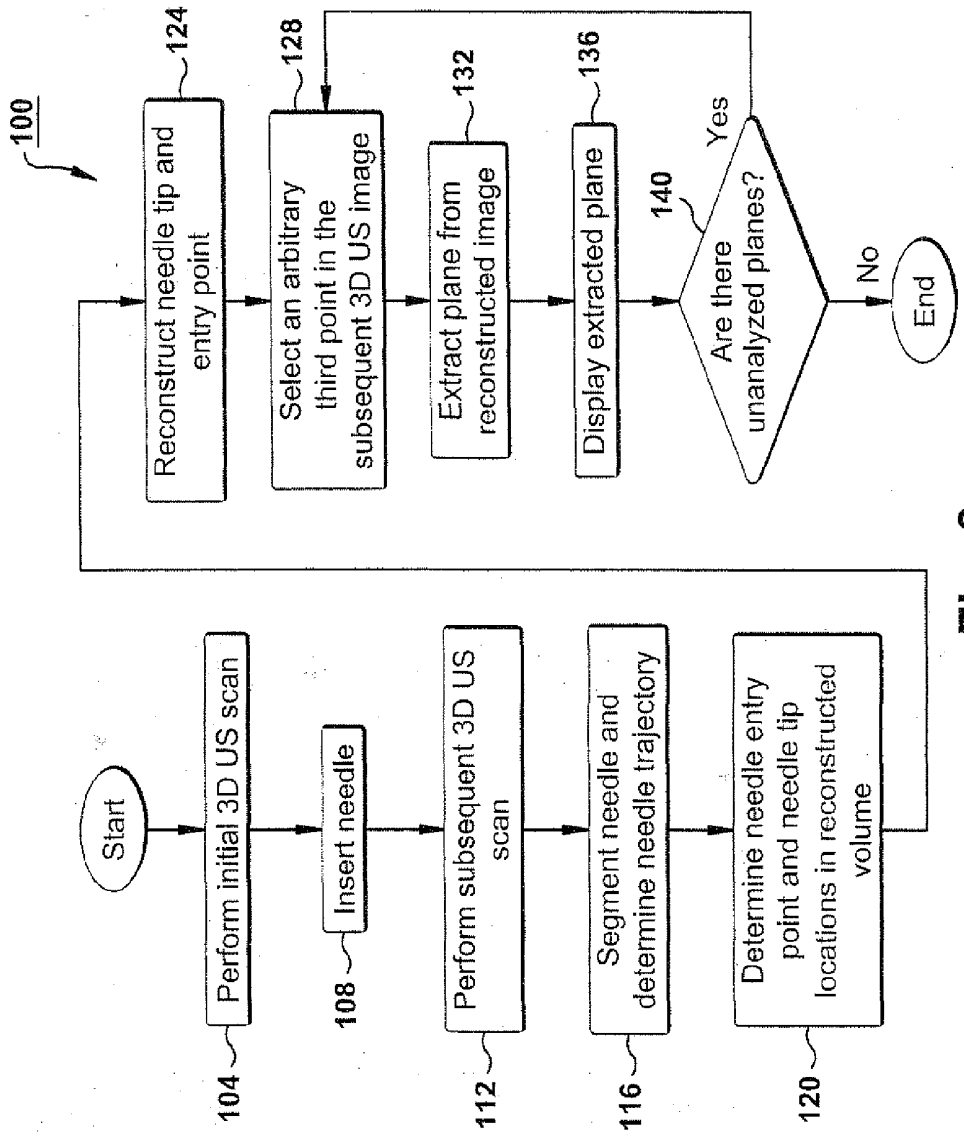
100
Start
Perform initial 3D US scan
104
Insert needle
108
Perform subsequent 3D US scan
112
Segment needle and determine needle trajectory
116
Determine needle entry point and needle tip locations in reconstructed volume
120
Reconstruct needle tip and entry point
124
Select an arbitrary third point in the subsequent 3D US image
128
Extract plane from reconstructed image
132
Display extracted plane
136
Are there unanalyzed planes?
140
Yes
No
End

Fig. 3

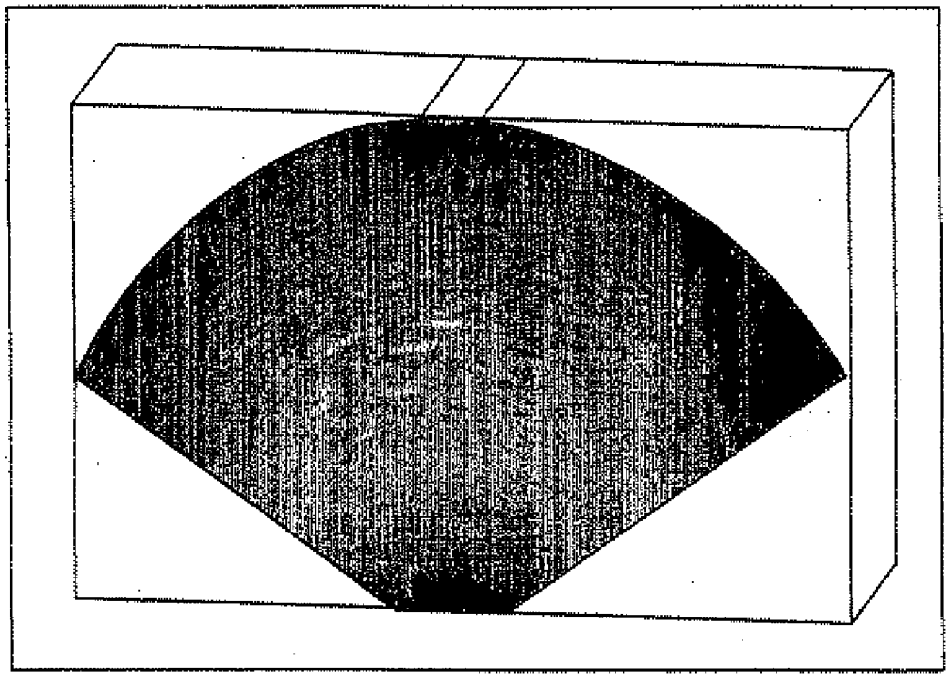

Fig. 4

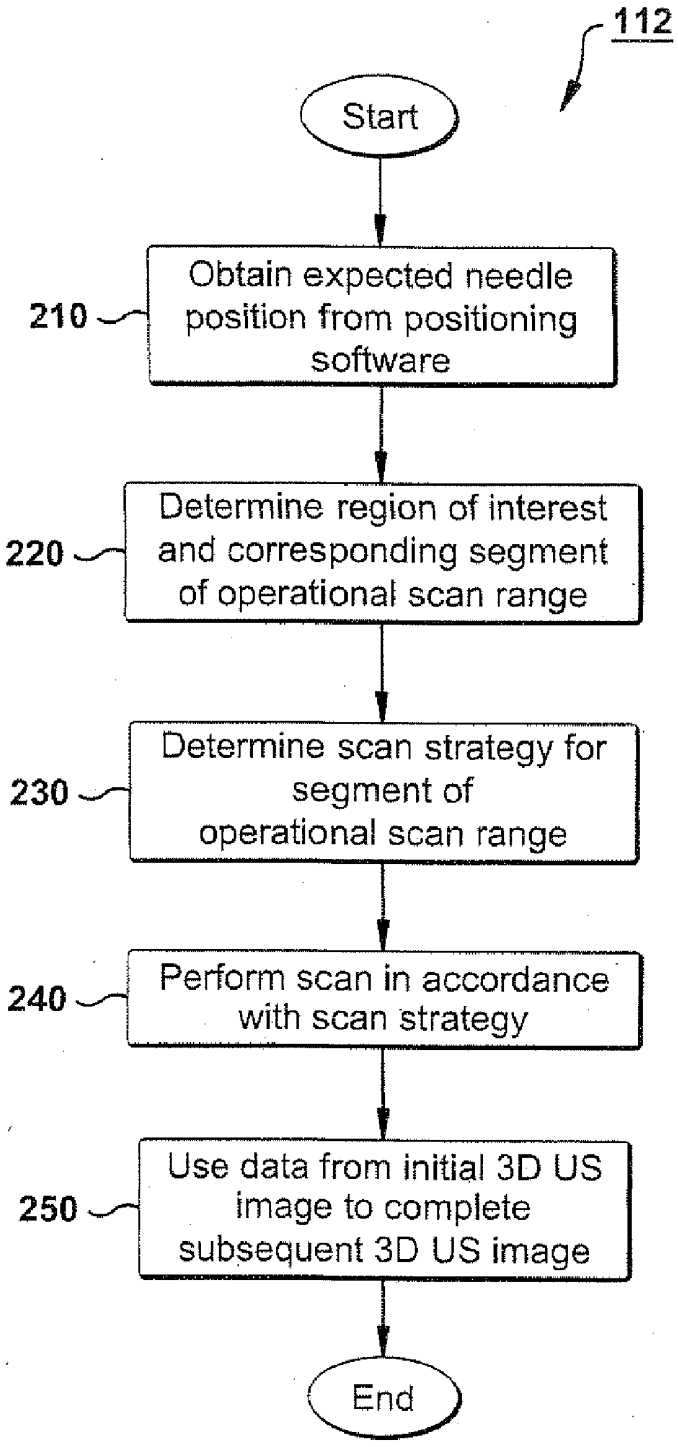
112
Start
Obtain expected needle position from positioning software
210
Determine region of interest and corresponding segment of operational scan range
220
Determine scan strategy for segment of operational scan range
230
Perform scan in accordance with scan strategy
240
Use data from initial 3D US image to complete subsequent 3D US image
250
End

Fig. 5

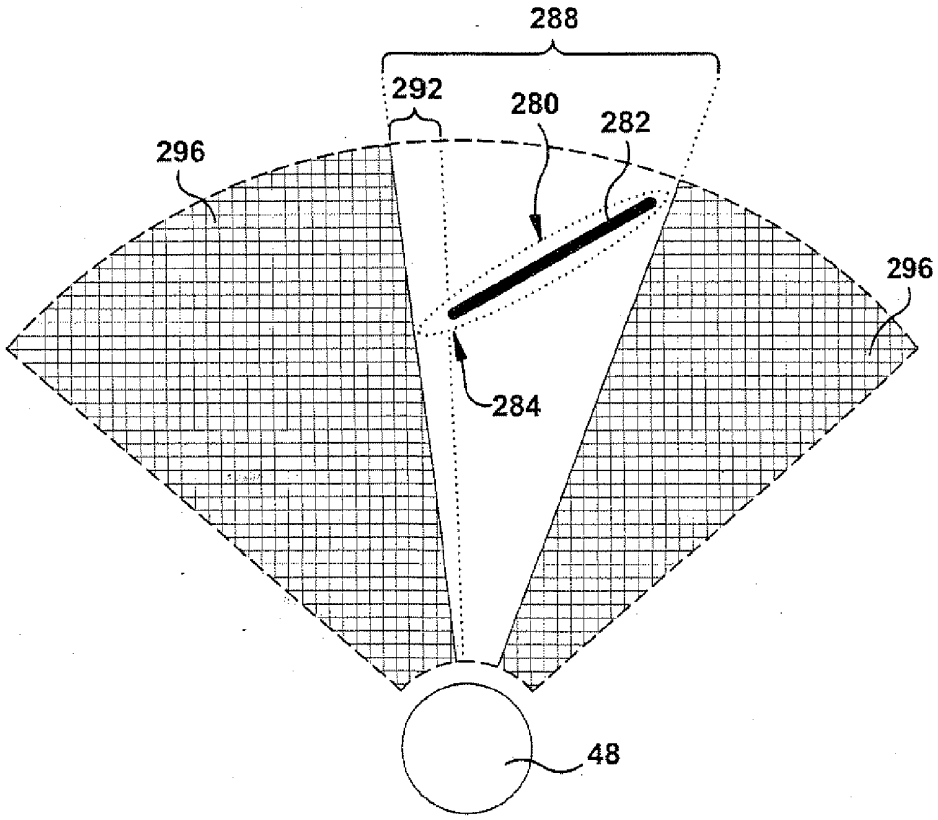

Fig. 6

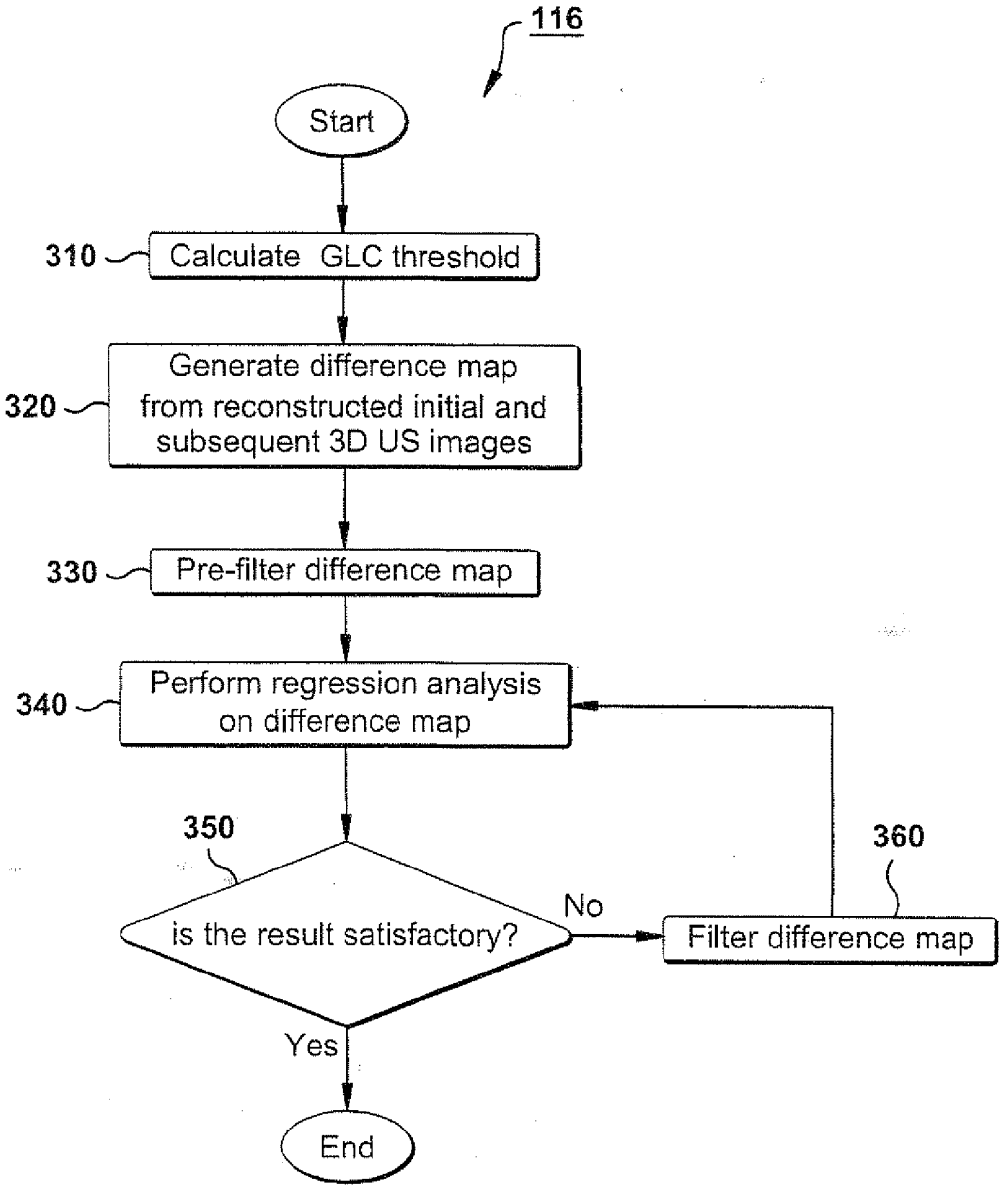
116
Start
310
Calculate GLC threshold
320
Generate difference map from reconstructed initial and subsequent 3D US images
330
Pre-filter difference map
340
Perform regression analysis on difference map
350
is the result satisfactory?
No
360
Filter difference map
Yes
End

Fig. 7

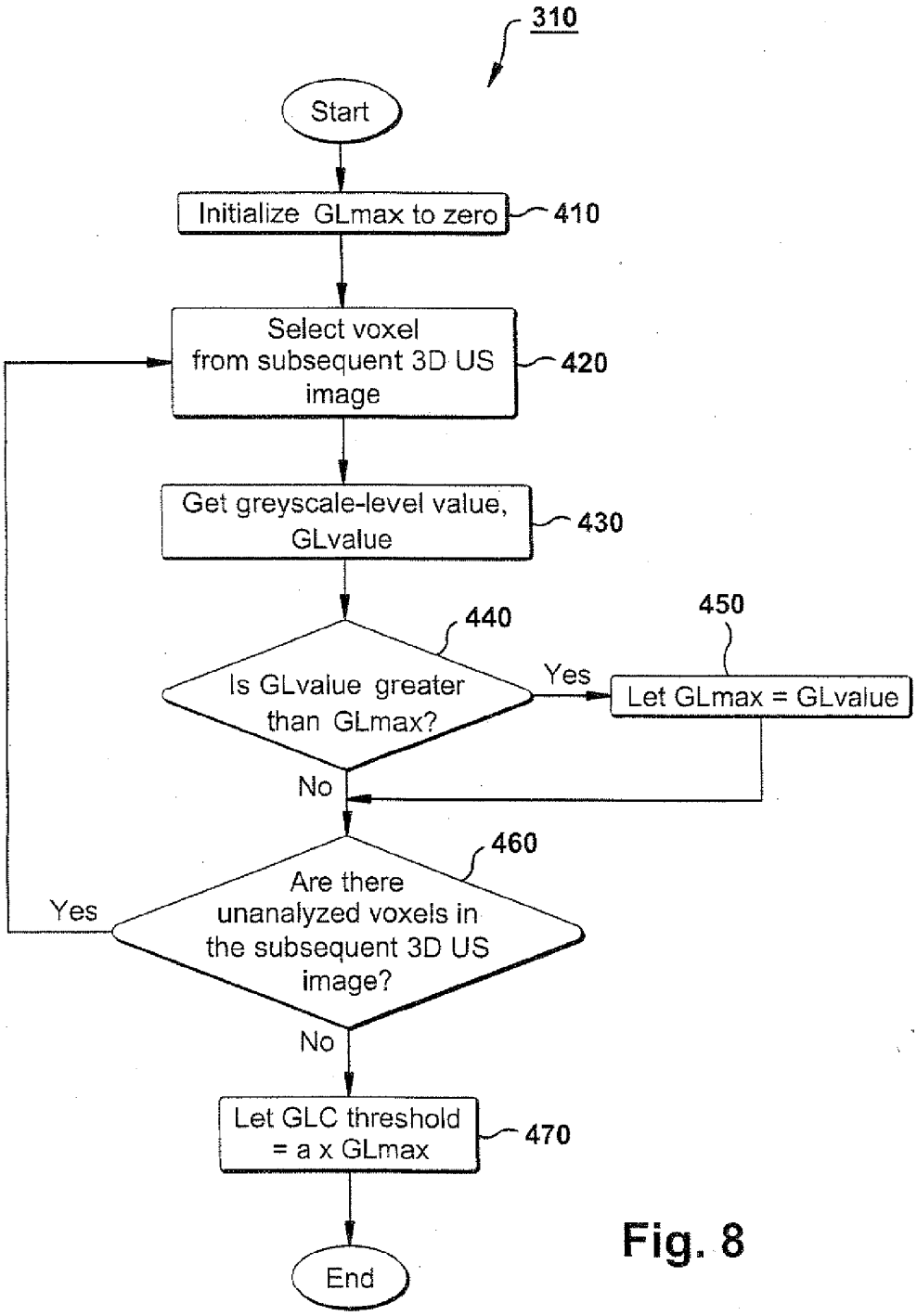
310
Start
Initialize GLmax to zero
410
Select voxel from subsequent 3D US image
420
Get greyscale-level value, GLvalue
430
440
Is GLvalue greater than GLmax?
Yes
450
Let GLmax = GLvalue
No
460
Are there unanalyzed voxels in the subsequent 3D US image?
Yes
No
Let GLC threshold = a x GLmax
470
End

Fig. 8

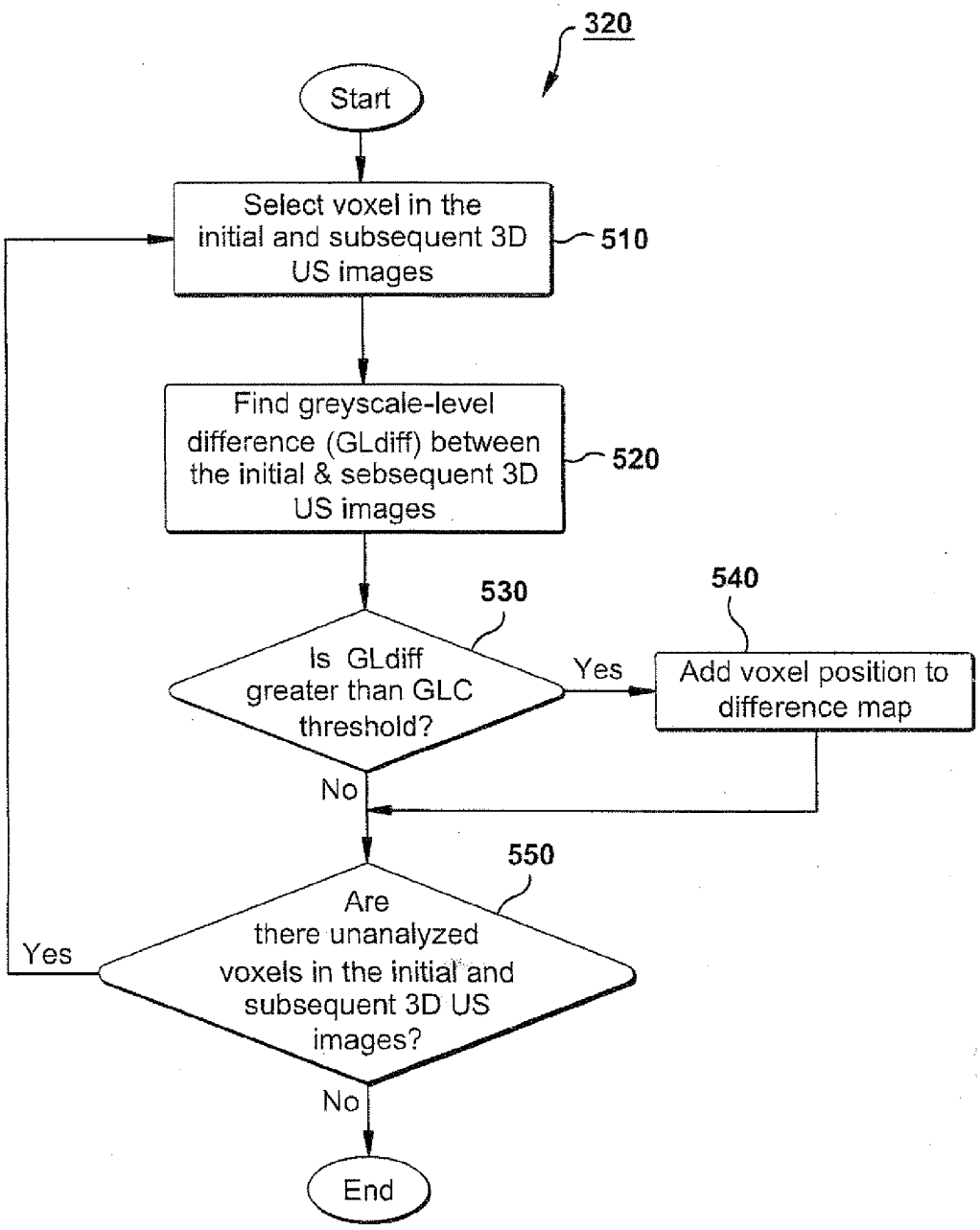
320
Start
Select voxel in the initial and subsequent 3D US images
510
Find greyscale-level difference (GLdiff) between the initial & sebsequent 3D US images
520
530
Is GLdiff greater than GLC threshold?
Yes
540
Add voxel position to difference map
No
550
Are there unanalyzed voxels in the initial and subsequent 3D US images?
Yes
No
End

Fig. 9

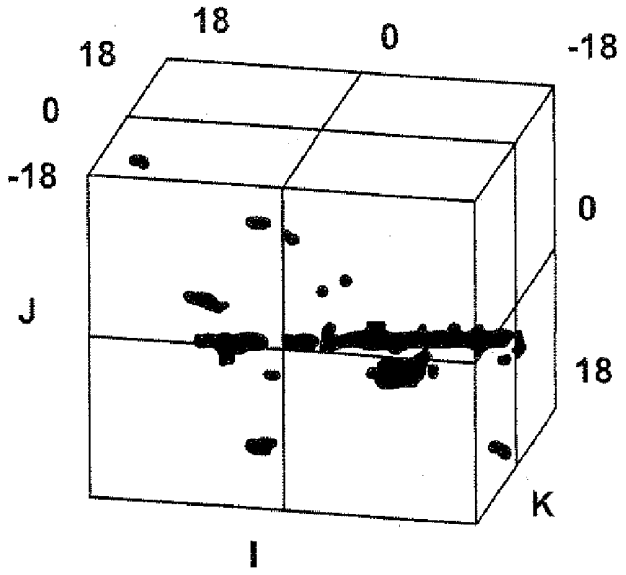

Fig. 10a

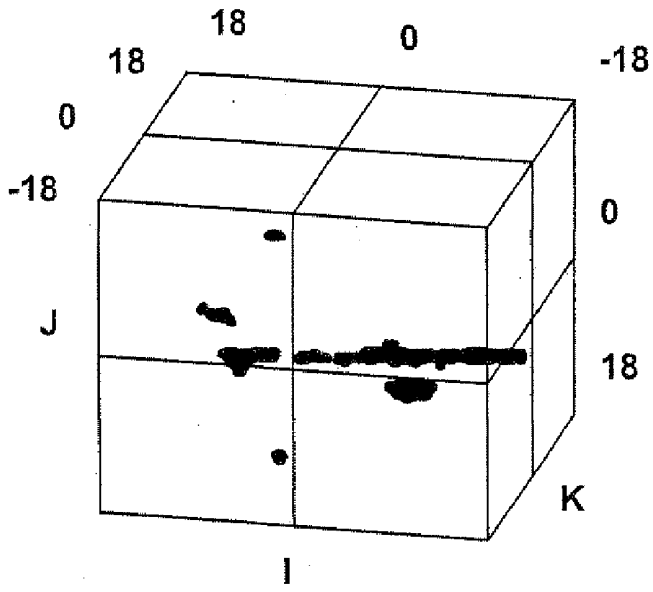

Fig. 10b

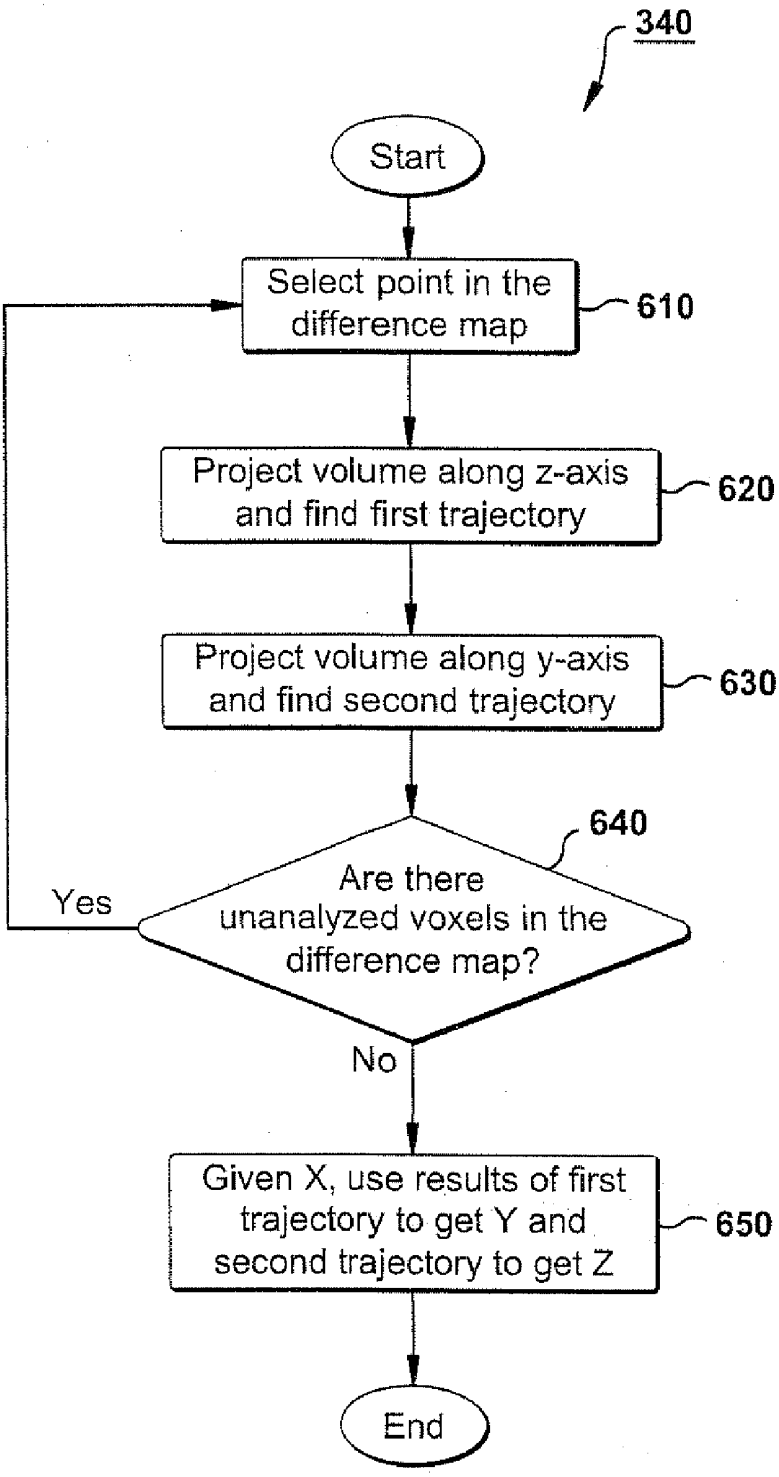
340
Start
Select point in the difference map
610
Project volume along z-axis and find first trajectory
620
Project volume along y-axis and find second trajectory
630
640
Are there unanalyzed voxels in the difference map?
Yes
No
Given X, use results of first trajectory to get Y and second trajectory to get Z
650
End

Fig. 11

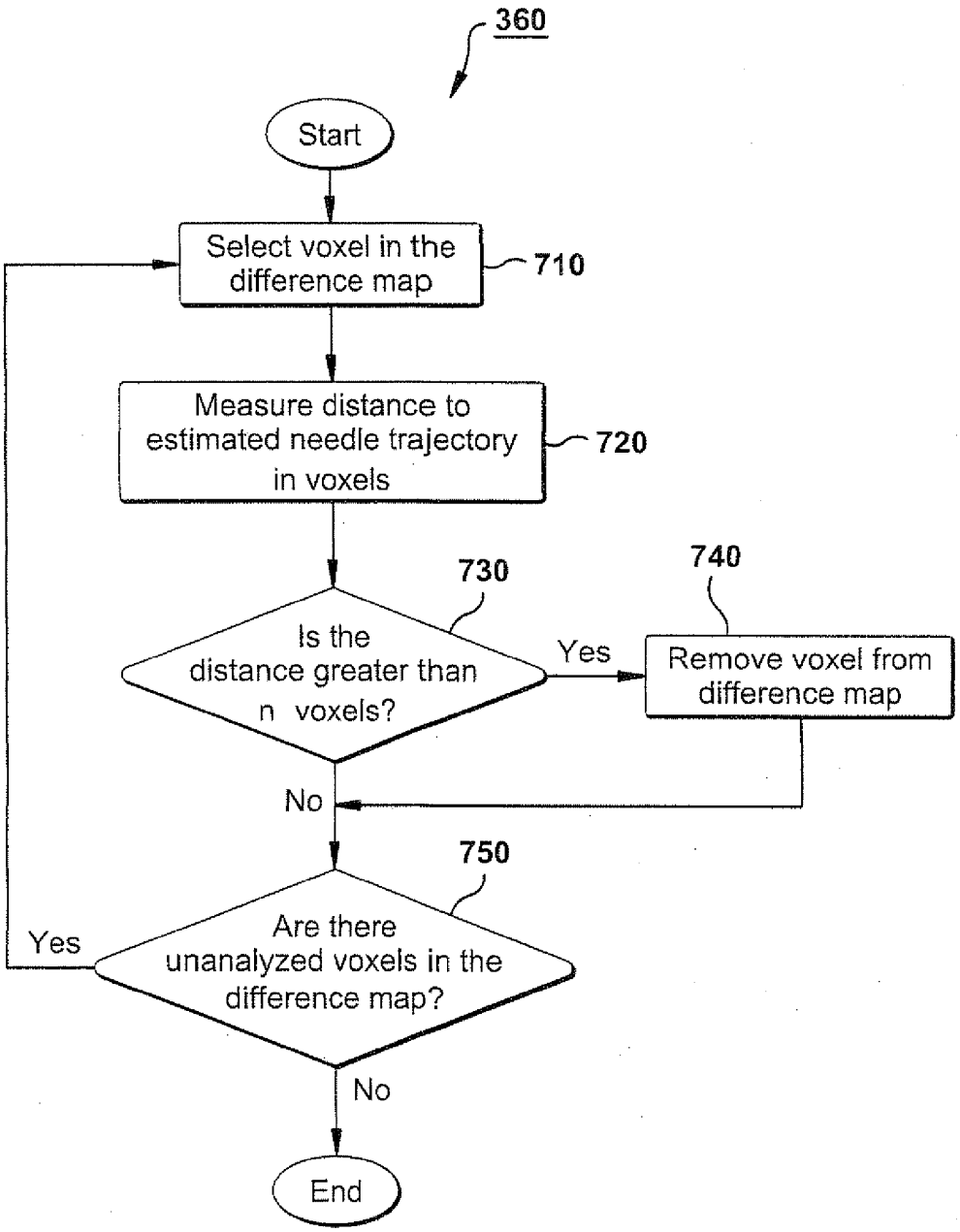
360
Start
Select voxel in the difference map
710
Measure distance to estimated needle trajectory in voxels
720
730
Is the distance greater than n voxels?
Yes
740
Remove voxel from difference map
No
750
Are there unanalyzed voxels in the difference map?
Yes
No
End

Fig. 12

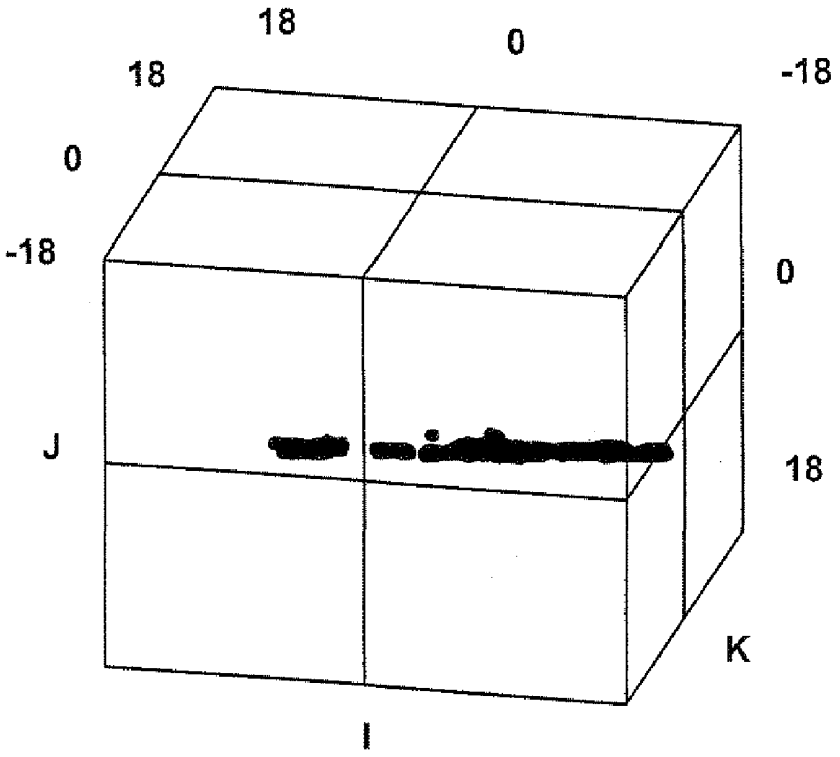

Fig. 13

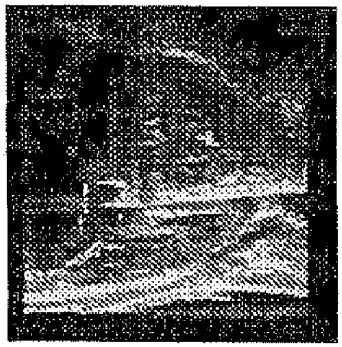

Fig. 14a

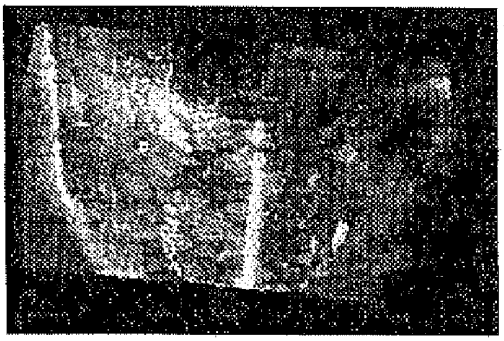

Fig. 14b

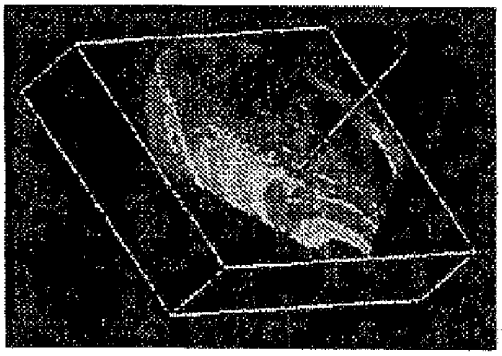

Fig. 14c

ULTRASOUND IMAGING SYSTEM AND METHODS OF IMAGING USING THE SAME

RELATED APPLICATIONS

[0001] This application is a divisional of U.S. patent application Ser. No. 12/706,476, filed Feb. 16, 2010, which is a continuation of U.S. patent application Ser. No. 10/585,984, filed Jul. 18, 2007 which corresponds to PCT International Application No. PCT/CA2005/000032, filed Jan. 12, 2005 and which claims benefit of U.S. Provisional Patent Application Ser. No. 60/535,825, filed Jan. 13, 2004. The subject matter of the aforementioned applications is incorporated herein by reference.

FIELD OF THE INVENTION

[0002] The present invention relates generally to imaging systems and, specifically, to an ultrasound imaging system and methods of imaging using the same.

BACKGROUND OF THE INVENTION

[0003] Ultrasound-guided interventional procedures such as breast biopsies and prostate brachytherapy are well-known. Needles can be inserted into the body and either obtain a biopsy sample or deliver a dose of a selected therapy. For biopsies, it is desirable to target a specific volume when obtaining a tissue sample. Where a dose is being administered to a target volume, it is desirable to track the precise location of the needle delivering the dose in real-time to ensure that the therapy is delivered according to plan.

[0004] Radioactive seeds can be used as a therapy to treat tumors in prostates. In order to ensure adequate coverage of the therapy, it is desirable to implant the seeds a pre-determined distance apart if the distance between the seeds is too large, tissue between the seeds may not receive the amount of therapy needed for the treatment. If, instead, the seeds are too closely positioned, the tissue can be over-exposed. Further, it is desirable to ensure that the implantation of the seeds is limited to the target volume in order to prevent the therapy from adversely affecting otherwise healthy tissue.

[0005] In robotic-aided interventional procedures, such as robot-aided and ultrasound-guided prostate brachytherapy as well as free-hand ultrasound-guided biopsy procedures, a needle is inserted free from parallel trajectory constraints. Oblique insertion of the needle, however, can result in the needle intersecting the two-dimensional ("2D") trans-rectal ultrasound ("TRUS") image and appearing as a point, leading to blind guidance.

[0006] Some investigators have developed automatic needle segmentation methods to locate needles for biopsies and therapy. These methods, however, require that the needle be completely contained in the 2D ultrasound ("US") image.

[0007] The general operation of ultrasound transducers has provided less-than-desirable image resolution in some instances. Image quality for less significant regions distal from the target volume or even along the shaft of the needles may not be as critical as for the region surrounding the needles. This is especially true for therapy where seeds are being implanted in a target volume. Current ultrasound techniques, however, are directed to the capture of generally evenly distributed images, regardless of the content of the volume targeted by the images.

[0008] It is, therefore, an object of the present invention to provide a novel method of imaging using an ultrasound imaging system.

SUMMARY OF THE INVENTION

[0009] In an aspect of the invention, there is provided a method of registering the position of an object moving in a target volume in an ultrasound imaging system, comprising:

[0010] capturing a first ultrasound image of a target volume;

[0011] capturing a second ultrasound image of said target volume after said capturing of said first ultrasound image; and

[0012] identifying the position of said object in said target volume using differences detected between said first and second ultrasound images.

[0013] In a particular aspect, a difference map of the differences between the first and second ultrasound images is generated. The difference map can be thresholded to identify significant changes between the first and second ultrasound images. In another particular aspect, the object is a needle, and the difference map is filtered to identify voxels in the difference map corresponding to a characteristic of the needle. In a further particular aspect, the first ultrasound image is captured prior to entry of the object in the target volume.

[0014] In another aspect of the invention, there is provided an ultrasound imaging system for registering the position of an object moving in a target volume, comprising:

[0015] a transducer for capturing a first ultrasound image and a second ultrasound image of a target volume; and

[0016] a processor for detecting differences between said first and second ultrasound images to identify the position of said object in said target volume.

[0017] In a particular aspect, the processor generates a difference map from the first and second ultrasound images identifying the differences therebetween. The processor can threshold the difference map to identify significant differences between the first and second ultrasound images.

[0018] In a further aspect of the invention, there is provided a method of imaging using an ultrasound imaging system operable to capture image data from a target volume, comprising:

[0019] determining a region of interest in the target volume;

[0020] determining a segment of an operational scan range of a transducer of said ultrasound imaging system encompassing said region of interest; and

[0021] focusing said ultrasound imaging system on said segment of said operational scan range during image capture.

[0022] In a particular aspect, the region of interest is an area of expected activity of an object. In another particular aspect, the object is a needle, and the region of interest includes the area along a trajectory of the needle beyond a tip of the needle. In a further particular aspect, the determining of the region of interest includes the expected position of a needle in the target volume. The transducer can be, for example, a rotational transducer. In still other particular aspects, the focusing includes capturing image data in the segment of the operational scan range at a greater scan density than outside of the segment of the operational scan range, or capturing image data only in the segment of the operational scan range.

[0023] In a still further aspect of the invention, there is provided an ultrasound imaging system, comprising:

[0024] a transducer for capturing ultrasound images of a target volume; and

[0025] a processor for determining a region of interest in the target volume, for determining a segment of an operational scan range of said transducer encompassing said region of interest, and for directing said transducer to focus on said segment of said operational scan range.

[0026] In a particular aspect, the processor determines an area of expected activity to determine the region of interest. In another particular aspect, the transducer is a rotational transducer and the processor determines an angular sector of the operational scan range of the rotational transducer. In a further particular aspect, the processor directs the transducer to capture image data in the segment of the operational scan range at a greater scan density than outside of the segment of the operational scan range. In a still further particular aspect, the processor directs the transducer to capture image data only in the segment of the operational scan range.

[0027] The invention enables the position of the needle to be accurately determined. By only analyzing image data that varies significantly between two ultrasound images, the needle can be readily differentiated from complex backgrounds in the ultrasound images. Further, by focusing on a segment of the operational scan range of the transducer of the ultrasound imaging system during image capture, more detailed image data can be captured around the needle to enable its position to be determined with a desired level of accuracy. This can be achieved without sacrificing the scanning speed in some cases.

BRIEF DESCRIPTION OF THE DRAWINGS

[0028] Embodiments will now be described, by way of example only, with reference to the attached Figures, wherein:

[0029] FIG. **1** is a schematic diagram of an ultrasound imaging system for imaging a target volume in a subject;

[0030] FIG. **2** shows a three-dimensional ("3D") TRUS transducer forming part of the ultrasound imaging system of FIG. **1** capturing a set of 2D US images of a needle;

[0031] FIG. **3** is a flow chart of the general method of operation of the system of FIG. **1**;

[0032] FIG. **4** shows a reconstructed 3D image generated from 2D ultrasound images captured by the TRUS transducer shown in FIG. **2**;

[0033] FIG. **5** is a flow chart illustrating the method of performing a subsequent 3D US scan;

[0034] FIG. **6** is a sectional view of a scan range corresponding to a region of interest determined using the method of FIG. **5**;

[0035] FIG. **7** is a flow chart that illustrates the method of segmenting a needle;

[0036] FIG. **8** is a flow chart that illustrates the method of determining the greyscale-level change threshold;

[0037] FIG. **9** is a flow chart that illustrates the method of generating a difference map;

[0038] FIGS. **10***a* and **10***b* show the difference map generated using the method of FIG. **9** before and after pre-filtration respectively;

[0039] FIG. **11** is a flow chart that illustrates the method of performing regression analysis;

[0040] FIG. **12** is a flow chart that better illustrates the method of filtering the difference map;

[0041] FIG. **13** shows the difference map of FIGS. **10***a* and **10***b* immediately prior to the performance of the final regression analysis; and

[0042] FIGS. **14***a* to **14***c* show various 2D US images generated using the ultrasound imaging system of FIG. **1**.

DETAILED DESCRIPTION OF THE EMBODIMENTS

[0043] The method of registering the position of an object such as a needle provides for the near real-time identification, segmentation and tracking of needles. It has a wide range of applications, such as biopsy of the breast and liver and image-guided interventions such as brachytherapy, cryotherapy, as well as other procedures that require a needle or needles to be introduced into soft tissues and be positioned accurately and precisely. The use of the method is described in robot-aided 3D US-guided prostate brachytherapy for the purpose of illustration.

[0044] Transperineal prostate brachytherapy provides an improved alternative for minimally-invasive treatment of prostate cancer. Pubic arch interference ("PAI") with the implant path, however, occurs in many patients with large prostates and/or a small pelvis. These patients cannot be treated with current brachytherapy using parallel needle trajectories guided by a fixed template, because the anterior and/or the antero-lateral parts of the prostate are blocked by the pubic bone.

[0045] To solve the PAI problems, it is desirable to free needle insertions from parallel trajectory constraints. Oblique trajectories allow patients with PAI to be treated with brachytherapy without first undergoing lengthy hormonal downsizing therapy. In addition, changes in the prostate size prior to implantation, where the therapy is determined in advance of the procedure, and during the implantation, due to swelling of the prostate, may require re-optimization of the dose plan. The combination of precision 3D TRUS imaging, dosimetry and oblique needle insertion trajectories can provide the tools needed for dynamic re-optimization of the dose plan during the seed implantation procedure by allowing dynamic adjustments of the needle position to target potential "cold spots". Cold spots are areas more than a desired distance from seed implantation locations, resulting in less-than-desired exposure. Further, the dosimetry can be dynamically adjusted to compensate for deviations in the actual needle trajectories or shifting in the target volume.

[0046] A 3D TRUS-guided robot-aided prostate brachytherapy system is shown generally at **20** in FIG. **1**. The system **20** includes a TRUS transducer **24** coupled to a motor assembly **28** that operates to control the longitudinal movement and rotation of the TRUS transducer **24**. The TRUS transducer **24** is also coupled to a conventional ultrasound machine **32** for displaying image data as it is captured by the TRUS transducer **24**. A video frame-grabber **36** is connected to the ultrasound machine **32** to capture image data therefrom. The video frame-grabber **36** preferably operates at 30 Hz or greater to provide rapidly updated ultrasound images.

[0047] A computer **40** is connected to the video frame-grabber **36** and retrieves ultrasound images from the memory of the video frame-grabber **36**. The computer **40** is coupled to a mover controller module ("MCM") **44** that is coupled to and controls the motor assembly **28**. The computer **40** is also connected to the TRUS transducer **24**. Further, the computer **40** is connected to a robot **48** having a needle driving assembly **52** and needle guide **56** for controlling movement of a needle **60**. The needle **60** is used to deliver therapy to a

prostate **64** of a patient. The robot **48** receives needle control commands from and transmits needle position information to the computer **40**.

[0048] The TRUS transducer **24** is operable to continuously capture radial 2D US images over a radial operational scan range. The MCM **44** which controls the TRUS transducer **24** is in communication with the computer **40** to receive TRUS control commands via the serial port of the computer **40**. The TRUS control commands direct the MCM **44** to control the motor assembly **28**. In turn, the motor assembly **28** controls the longitudinal movement and rotation of the TRUS transducer **24**. Additionally, the TRUS control commands control the timing of image data capture of the TRUS transducer **24**.

[0049] The needle driving assembly **52** includes a robotic arm with six degrees-of-freedom. The degrees-of-freedom correspond to translations of the needle **60** in three dimensions and rotation of the needle **60** about three orthogonal axes. In this manner, the needle **60** can be positioned in a wide variety of orientations. The needle guide **56** is a one-holed template that is used to stabilize lateral movement of the needle **60** during insertion.

[0050] The computer **40** is a personal computer having a processor that executes software for performing 3D image acquisition, reconstruction and display. The processor also executes software for determining dosimetry of a selected therapy, and for controlling the TRUS transducer **24** and the robot **48**. The software executed by the processor includes TRUS controller software, positioning software, imaging software, 3D visualization software and dose planning software.

[0051] The TRUS controller software generates TRUS control commands for directing the MCM **44**, thereby controlling the longitudinal and rotational movement and the image data acquisition timing of the TRUS transducer **24**.

[0052] The positioning software generates needle control commands to control movement of the needle driving assembly **52** of the robot **48**. The positioning software can direct the robotic arm to move in terms of world or tool coordinate systems. The world coordinate system is fixed to the ground, whereas the tool coordinate system is fixed to the robotic arm. Further, the positioning software can direct the needle driving assembly **52** to control the longitudinal movement of the needle **60**.

[0053] The imaging software captures, analyzes and processes ultrasound images using the image data retrieved from the memory of the video frame-grabber **36**. The positioning software provides needle position information using the selected coordinate system. In turn, the imaging software directs the TRUS controller software to vary the operation of the TRUS transducer **24** as will be explained.

[0054] The 3D visualization software renders 3D images to be presented on a display (not shown) of the computer **40** using the image data captured and processed by the imaging software. In particular, the 3D visualization software generates three orthogonal views of the target volume: two that are co-planar to the needle **60** and a third that generally bisects the needle **60**.

[0055] The dose planning software performs precise image-based needle trajectory planning. In addition, the dose planning software provides planned needle trajectory information to the 3D visualization software so that the planned needle trajectory can be overlaid atop the US images on the display. The actual needle trajectory can then be viewed in relation to the planned needle trajectory. The dose planning software can also receive and process the US images from the imaging software and dynamically re-determine the dosimetry based on the actual needle trajectory and seed implantation locations.

[0056] Prior to use, the positioning software controlling movement of the robot **48**, the needle driving assembly **52** and, thus, the needle **60**, and the imaging software are calibrated. During calibration, the mapping between the selected coordinate system of the positioning software and the 3D TRUS image coordinate system is determined and synchronized. In this manner, the imaging software can be made aware of the expected position of the needle **60** before detection via imaging.

[0057] By unifying the robot **48**, the TRUS transducer **24** and the 3D TRUS image coordinate systems, the position of the template hole of the needle guide **56** can be accurately related to the 3D TRUS image coordinate system, allowing accurate and consistent insertion of the needle via the hole into a targeted position in a prostate along various trajectories including oblique ones. Further, the operation of the TRUS transducer **24** can be varied to focus its attention on the expected position of the needle **60**.

[0058] FIG. **2** shows the 3D TRUS transducer **24** capturing a set of 2D US images. As the TRUS transducer **24** is rotated by the MOM **44**, it captures image data to generate a series of 2D images **68**. The 2D images **68** are captured at generally regular intervals during rotation of the TRUS transducer **24**. Initially, the TRUS transducer **24** captures a 2D image **68** every one degree of rotation and rotates through 100 degrees, thereby capturing one hundred and one 2D images **68**. The captured 2D images **68** are fanned radially in relation to the TRUS transducer **24**. The needle **60** is shown having an oblique trajectory in relation to the 2D images **68**, and intersects two or more of the 2D images **68**.

[0059] As will be understood, insertion of the needle **60** along an oblique trajectory results in the intersection of the 2D TRUS image planes. As a result, the needle **60** only appears as a point in the captured 2D US images.

[0060] A near real-time method **100** for identification, segmentation and tracking of needles will now be described with reference to FIG. **3**. The method **100** enables the tracking of the needle **60** even if the needle **60** is not coplanar and, thus, exits a 2D US image plane as a result of an oblique insertion. The method can also be used for the identification, segmentation and tracking of needles if they are completely contained in a 2D US image plane. To perform near real-time needle segmentation for an oblique trajectory, capture of two 3D US images is required. A 3D US image is comprised of two or more 2D US images that are offset. Note, that if the needle **60** is coplanar with a 2D US image, then two 2D US images can generally be used, but the procedure is unchanged.

[0061] The initial 3D US image is obtained by scanning the prostate (tissue) to obtain a set of 2D US images before the needle is inserted. This 3D US image establishes a baseline or control against which other images will be compared. A subsequent 3D US image is then acquired by scanning only the region containing the needle. It is to be understood that the second 3D US image may not be, in fact, the next 3D US image captured after the first, but refers to any subsequently-captured 3D US image. The method, as described, is used to identify, segment and track the needle in each subsequent 3D US image captured after the first 3D US image is captured.

Each new 3D US image is compared to the initial image to identify the position of the needle at that time.

[0062] The method **100** commences with the performance of an initial 3D US scan (step **104**). The needle **60** is then inserted into the target volume (step **108**). Next, a subsequent 3D US scan is performed (step **112**). The needle **60** is segmented to distinguish its location using the initial and subsequent 3D US images (step **116**). The needle trajectory is then determined (step **120**). Once the needle trajectory has been determined, the needle tip and needle entry point locations within the reconstructed volume are determined (step **124**). The needle tip and entry point locations are then reconstructed (step **128**). An arbitrary third point in the target volume is selected (step **132**). The plane defined by the needle tip and entry points and the arbitrary third point is extracted from the reconstructed 3D image (step **136**). Next, the extracted plane is displayed (step **140**). It is then determined if there are any remaining unanalyzed planes (step **144**). If there are, the method **100** returns to step **132**, at which another arbitrary point is selected. If, instead, all of the desired planes have been analyzed, the method **100** ends.

[0063] During the performance of the initial 3D US scan at step **104**, the MCM **44** and motor assembly **28** causes the TRUS transducer **24** to rotate about its long axis over about 100 degrees while image data corresponding to 2D US images is captured at one degree intervals. The image data corresponding to the 2D US images is then transmitted to the computer **40** to be digitized by the video frame grabber **36** and registered by the imaging software.

[0064] The acquired 2D US images are processed by the imaging software as they are collected. The 2D US images correspond to planes radially extending from the central axis of rotation of the TRUS transducer **24**. Accordingly, the 3D volume is reconstructed by translating and rotating the 2D US images with respect to one another. The reconstructed 3D volume consists of an array of voxels, or 3D pixels. The voxels are typically cubic (but can also be rhomboidal) and are arranged according to a 3D Cartesian system. Each voxel is assigned a greyscale-level value based on the greyscale-level values of the pixels in the translated 2D images adjacent to it.

[0065] FIG. **4** illustrates a 3D US image reconstructed from the set of 2D US images. As can be seen, the 3D US image has a fan profile corresponding to the volume imaged by the TRUS transducer **24**. The acquired 2D US images are reconstructed into a 3D US image by the imaging software. The 3D visualization software then generates a view of the 3D US image, and provides a multi-planar 3D display and volume rendering, as well as an extensive set of measurement tools. The 3D US image is then presented for viewing on the display of the computer **40**. As each new 2D US image is acquired by the TRUS transducer **24** during its rotation, the 3D visualization software dynamically updates the 3D image presented on the display.

[0066] During the performance of the subsequent 3D US scan at step **112**, a region of interest is identified, and the ultrasound imaging system **20** is focused on a segment of an operational scan range of the TRUS transducer encompassing the region of interest in a target volume. In particular, the TRUS transducer is focused on the segment to capture images of the expected position of the needle **60**. While the expected position of the needle **60** in the 3D US images can be determined based on the needle position coordinates provided by the positioning software, needle deviations in the 3D US images can occur for a number of reasons. These include slight bending of the needle **60** as it is inserted and shifting in the target volume. By obtaining a new 3D US image, the actual position of the needle **60** can be more precisely determined.

[0067] FIG. **5** better illustrates the performance of the subsequent 3D US scan. The expected needle position is obtained from the positioning software (step **210**). The region of interest is determined based on the expected position of the needle, and a corresponding segment of the operational scan range of the TRUS transducer **24** is determined (step **220**). Next, a scan strategy for the segment of the operational scan range is determined (step **230**). In determining the scan strategy for the segment of the operational scan range at step **230**, the positions of 2D US images to be acquired is determined. In particular, a set of 2D US images are planned at one-half degree intervals along the angular width of the scan region of interest. A scan is then performed in accordance with the scan strategy (step **240**). Data from the initial 3D US image is then used to complete the 3D US image (step **250**).

[0068] During the determination of the region of interest at step **220**, the region of interest is selected to include the expected needle position obtained during step **210**. Where the needle has yet to be inserted/detected, the region of interest is defined to be an area around the expected needle entry point. If, instead, the needle was at least partially inserted/detected at the time of the last 3D US scan, the region of interest is determined to include the original needle position plus a distance along the needle trajectory beyond the needle tip as will be described.

[0069] The region of interest is then reverse-mapped onto the operating coordinates of the TRUS transducer **24** and is used to determine a segment of the operational scan range of the TRUS transducer **24** that encompasses the region of interest at step **230**. In particular, the segment of the operational scan range is selected to correspond to an angular sector of the operational scan range of the TRUS transducer **24** that encompasses the region of interest. Where the needle is inserted along an oblique trajectory and, consequently, intersects a number of 2D US images at points, the angular width of the sector is selected to sufficiently cover the region of interest plus five degrees of rotation to cover the distance along the needle trajectory beyond the needle tip.

[0070] FIG. **6** is an end-view of the TRUS transducer **24** and the segment of the operational scan range selected during step **220** for the needle when it is inserted along an oblique trajectory. A region of interest **280** encompasses an expected needle position **282** and extends a distance past the expected needle tip position **284**. A segment of the operational scan range **288** corresponding to the sector encompasses the region of interest **280**. The segment of the operational scan range **288** includes a five-degree margin **292** to capture the region of interest extending along the needle trajectory beyond the expected needle tip position **284**. Two background areas **296** of the operational scan range of the TRUS transducer **24** flank either side of the sector.

[0071] During the completion of the subsequent 3D US image at step **250**, data from the initial 3D US image is used to fill in the background areas. As the scan strategy can exclude the capture of some or all image data from the background areas, image data from the initial 3D US scan is used to fill in any image data required in the subsequent 3D US

image. The image data in the background areas is not expected to change and can, thus, be borrowed from the initial 3D US image.

[0072] By modifying the behavior of the TRUS transducer **24** to focus on the region of interest, more detailed information can be captured around the tip of the needle **60** on a near real-time basis. Further, by reducing the scanning density for the other areas, the additional time required to scan the region of interest can be compensated for.

[0073] After the initial and subsequent 3D US scans have been completed, the needle **60** is segmented at step **116**. The subsequent 3D US image is compared to the initial 3D US image, and the needle position within the subsequent 3D US image, including the needle tip and entry point location, is determined. The needle **60** will show up as voxels with a greyscale-level change that exceeds a threshold value between the initial and subsequent 3D US images. There can be, however, other voxels with a greyscale-level change that exceeds the threshold value that do not, in fact, represent the needle, but may represent, for example, calcifications in the prostate. In order to permit better identification of the actual needle, the system **20** attempts to identify and discard these other voxels.

[0074] FIG. **7** better illustrates the method of needle segmentation at step **116**. The method commences with the calculation of a greyscale-level change threshold (step **310**). A difference map is then generated from the initial and subsequent 3D US images (step **320**). Next, the difference map is pre-filtered (step **330**). Regression analysis is performed on the difference map to identify the needle (step **340**). The result of the regression analysis is then analyzed to determine if it is satisfactory (step **350**). If the results are determined to be unsatisfactory, the difference map is filtered (step **360**), and the method returns to step **340**, where regression analysis is again performed on the filtered image. The filtering of the difference map and the regression analysis is repeated until all of the voxels in the difference map are within a prescribed range from the regression line. As the filtering removes outlying voxels, their effect on the linear regression is removed, thereby allowing the needle trajectory to be more accurately estimated. Reiterative filtration of the difference map is performed to obtain a desired level of confidence in the estimated needle trajectory. Once the result of the regression analysis is deemed to be satisfactory at step **350**, the method ends.

[0075] FIG. **8** better illustrates the calculation of the greyscale-level change threshold at step **310**. A greyscale-level change threshold value, GLC threshold, is used to reduce the number of voxels to be analyzed in the 3D US images and to obtain candidate needle voxels. To determine the threshold value, the maximum greyscale-level value, GL_{max}, in the subsequent 3D US image is first determined by examining each voxel in the image, and then GL_{max} is multiplied by a constant.

[0076] The calculation of GLC threshold commences with the setting of GL_{max} to zero (step **410**). A voxel is then selected from the subsequent 3D US image (step **420**). The greyscale-level value, GL_{value}, of the selected voxel is determined (step **430**). The greyscale-level value of the selected voxel, GL_{value}, is then compared to the maximum greyscale-level value, GL_{max} (step **440**). If the greyscale-level value of the selected voxel, GL_{value}, is greater than the maximum greyscale-level value, GL_{max}, the value of GL_{max} is set to GL_{value} (step **450**). It is then determined whether there are any unanalyzed voxels remaining in the subsequent 3D US image (step **460**). If there are, the method returns to step **420**, where another voxel is selected from the subsequent 3D US image. If, instead, it is determined at step **460** that there are no remaining unanalyzed voxels in the subsequent 3D US image, the greyscale-level change threshold value is calculated as follows:

$$GLC\ \text{threshold} = a \times GL_{max} \quad \text{(Eq. 1)}$$

where 0<a<1. A value for a of 0.5 provides desirable results.

[0077] FIG. **9** better illustrates the generation of a difference map during step **320** using the threshold calculated during step **310**. The difference map is a registry of candidate needle voxels that represent an area of the same size as the initial and subsequent 3D US images. Initially, the greyscale-level value of each voxel in the initial 3D US image is compared to that of its counterpart in the subsequent 3D US image, and the difference is determined:

$$GLC(i,j,k) = \text{post}GL(i,j,k) - \text{pre}GL(i,j,k) \quad \text{(Eq. 2)}$$

where preGL(i,j,k) and postGL(i,j,k) are the greyscale-level values of voxels at location (i,j,k) in the initial and subsequent 3D US images respectively, and GLC(i,j,k) is the greyscale-level change.

[0078] Those voxels in the subsequent 3D US image whose greyscale-level values exceed those of their counterpart in the initial 3D US image are deemed to have changed significantly and are registered in the difference map. That is,

$$(i_m, j_m, k_m) \in 3D\ DM, \text{ where } GLC(i_m j_m k_m) > GLC\ \text{threshold} \quad \text{(Eq. 3)}$$

for m=1, 2, . . . , n, where n is the number of points included in the 3D difference map. The remaining voxels having greyscale-level values that do not exceed those of their counterpart in the initial 3D US image are deemed to have changed insignificantly and are not added to the difference map.

[0079] The method of generating the difference map begins with the selection of a voxel in the subsequent 3D US image and its counterpart in the initial 3D US image (step **510**). The greyscale-level difference, GLdiff, between the voxels of the initial and subsequent 3D US images is found (step **520**). The greyscale-level difference, GLdiff, is compared to the greyscale-level change threshold, GLC threshold, to determine if it exceeds it (step **530**). If it is determined that the greyscale-level difference, GLdiff, exceeds the greyscale-level change threshold, GLC threshold, the position of the voxel is added to the difference map (step **540**). It is then determined whether there are any remaining unanalyzed voxels in the initial and subsequent 3D US images (step **550**). If it is determined that there are unanalyzed voxels remaining in the initial and subsequent 3D US images, the method returns to step **510**, where another pair of voxels is selected for analysis. If, instead, it is determined that all of the voxels in the initial and subsequent 3D US images have been analyzed, the method of generating the difference map ends.

[0080] During pre-filtration of the difference map at step **330**, voxels registered in the difference map are analyzed to remove any voxels that are deemed to be noise. In the system **20**, the 3D image is advantageously reconstructed on demand and, therefore, access to the original acquired image data is available.

[0081] Voxels are identified and analyzed to determine whether they correspond to a characteristic of the needle. Since the image of the needle is expected to extend along the 3D scanning direction, voxels representing the needle are assumed to be generally adjacent each other along this direction. Other voxels in the difference map that are more than a pre-determined distance along this direction from other voxels are deemed to be noise and removed. That is, assuming that k is the direction along which the needle is expected to extend, voxels are removed from the difference map as follows:

$$(i_m, j_m, k_m) \notin 3D\ DM, \quad \text{(Eq. 4)}$$

$$\text{where } \bigcup_{m=1}^{P} GLC(i_m, j_m, k_m \pm s) < GLC \text{ threshold}$$

where, s=1, 2, . . . , $^{P}/_{2}$, and P is the number of voxels surrounding voxel (i_m,j_m, k_m) in the k-direction. A value for P of 4 provides desirable results.

[0082] FIGS. **10***a* and **10***b* show the difference map prior to and after pre-filtration respectively. As can be seen, spurious voxels not occurring in clusters extending along the same path as the needle are removed during pre-filtration.

[0083] Once the difference map has been pre-filtered, regression analysis is performed on the difference map at step **340**. During this analysis, a line is fit to the voxels in the difference map using linear regression analysis. The equation of the line determined from the difference map using linear regression analysis provides the estimated trajectory for the needle.

[0084] FIG. **11** better illustrates the performance of the regression analysis on the difference map at step **340**. A voxel registered in the difference map is selected (step **610**). The volume is projected along the z-axis to find a first trajectory (step **620**). Next, the volume is projected along the y-axis to find a second trajectory (step **630**). It is then determined if there are any unanalyzed voxels in the difference map (step **640**). If it is determined that there are unanalyzed voxels in the difference map, the method returns to step **610**, where another voxel is selected in the difference map for analysis. If, instead, all of the voxels in the difference map have been analyzed, the results of the first trajectory are used to obtain y and the results of the second trajectory are used to obtain z, given x (step **650**). Once (x,y,z) has been determined, the method **240** ends.

[0085] If it is determined at step **350** that the linear regression is unsatisfactory, the difference map is filtered at step **360**.

[0086] FIG. **12** better illustrates the filtering of the difference map. During the filtering of the difference map, spurious voxels that are further than a predetermined distance from the estimated trajectory of the needle determined during step **340** are removed.

[0087] The method of filtering the difference map commences with the selection of a voxel in the difference map (step **710**). The distance to the estimated needle trajectory is measured in voxels (step **720**). A determination is then made as to whether the distance between the voxel and the estimated needle trajectory is greater than a pre-determined distance limit (step **730**). It has been found that filtering out voxels further than five voxels in distance from the segmented needle trajectory provides desirable results. If the distance determined is greater than the pre-determined distance limit, the voxel is removed from the difference map (step **740**). Then, it is determined if there are any unanalyzed voxels remaining in the difference map (step **750**). If there are, the method returns to step **710**, wherein another voxel in the difference map is selected for analysis. If, instead, all of the voxels in the difference map have been analyzed, the method of filtering the difference map ends.

[0088] FIG. **13** shows the difference map of FIGS. **10***a* and **10***b* after filtration at step **360** and immediately prior to the final regression calculation. As can be seen, the difference map is free of spurious voxels distant from the visible needle trajectory.

[0089] As mentioned previously, once the needle trajectory has been determined, the needle entry point and needle tip locations are reconstructed at step **124**. The needle entry point is determined to be the intersection of the needle trajectory and the known entry plane. The needle tip is deemed to be the furthest needle voxel along the needle trajectory.

[0090] After the needle tip and entry point have been reconstructed, an arbitrary third point in the subsequent 3D US image is selected at step **128**. To extract any plane containing the needle, the segmented needle entry point, needle tip point and a third point within the subsequent 3D US image are used to define a specific plane that is coplanar with the needle (i.e., contains the needle lengthwise). The location of the arbitrary point determines whether the plane will be sagital-oblique or coronal oblique. For a sagital-oblique plane, the arbitrary point is picked on a line going through the needle entry point and parallel to the y-axis. For a coronal-oblique plane, the arbitrary point is picked on a line going through the needle entry point and parallel to the x-axis.

[0091] The data occurring along the plane in the 3D US image is extracted at step **132** to permit generation of a 2D US image of the plane. In this way, the oblique saggital, coronal and transverse views with the needle highlighted can be extracted and displayed.

[0092] Once the plane is extracted, the 2D US image of the plane is presented on the display of the computer **40** at step **136**. The location of the needle **60** in the 2D US image is demarcated using a colored line in the greyscale image to facilitate visual identification of the needle.

[0093] It is then determined whether there remain any unanalyzed planes at step **140**. As three planes are displayed by the computer **40** at the same time, the process is repeated twice to obtain the other two planes. The first plane selected for analysis is the saggital plane and the other two planes are orthogonal to the first plane. If there are, the method returns to step **128**, where another arbitrary point is selected to define another plane. Otherwise, the method **100** ends.

[0094] FIGS. **14***a* to **14***c* show a 2D US image obtained using the method **100** during a patient's prostate cryotherapy procedure, demonstrating that the needle can be tracked as it is being inserted and orthogonal views can be displayed for the user during the insertion procedure.

Evaluation

Experimental Apparatus

[0095] The accuracy and variability of the needle segmentation and tracking technique was tested using images acquired by scanning phantoms. Referring again to FIG. **1**, the robot **48** shown was used to insert the needle **60** at known angles, including oblique trajectories with respect to the TRUS image plane.

[0096] The needle used in these experiments was a typical 18-gauge (i.e., 1.2 mm in diameter) prostate brachytherapy needle. The two US tissue-mimicking phantoms were made of agar, using a recipe developed by D. W. Ricky, P. A. Picot, D. C. Christopher, A. Fenster, *Ultrasound Medical Biology*, 27(8), 1025-1034, 2001, and chicken breast tissues. TRUS images were obtained using an 8558/S side-firing linear array transducer with a central frequency of 7.5 MHz, attached to a B-K Medical 2102 Hawk US machine (B-K, Denmark). The computer was a Pentium Ill personal computer equipped with a Matrox Meteor II video frame grabber for 30 Hz video image acquisition.

Algorithm Execution Time

[0097] Execution time is dependent on the 3D scanning angular interval and the extent of the region to be investigated. To evaluate the execution time of the disclosed method of

needle segmentation the initial 3D US scan was performed, and then the needle was inserted. After needle insertion, the phantom was scanned again, and the needle was segmented. A software timer was used to measure the time elapsed during the execution of the segmentation.

Accuracy Test

[0098] To test the accuracy of the method, the robot was used to guide the needle insertion into the phantom at known angles. The angulation accuracy of the robot was evaluated to be 0.12±0.07 degrees.

[0099] First, the robot was used to guide the needle insertion along a trajectory parallel to the TRUS transducer **24**, hereinafter referred to as the zero (0) degree orientation. Since the needle could be verified by observing the needle in the real-time 2D US image, this trajectory was assumed to be correct. As a result, oblique trajectory accuracy measurements could be made with respect to the zero degree trajectory. The positions of the needle tip and the needle entry point were then found for the zero degree trajectory using the method described above. The robot **48** was used to insert the needle at different angles (+5, +10, +15, −5, −10 and −15 degrees) with respect to the zero degree trajectory. For each insertion, the positions of the needle tip and the needle entry point were found. The corresponding segmented needle vectors through the needle entry point and needle tip were determined by using the following formula:

$$\cos\theta_{alg} = \frac{\vec{A}\cdot\vec{B}}{|\vec{A}||\vec{B}|} \quad \text{(Eq. 5)}$$

where $\vec{A}$ is the segmented needle vector for the zero degree trajectory; $\vec{B}$ is the segmented needle vector for the insertion at any other angle; θ_{alg} is the angle derived from the segmentation algorithm. The accuracy of the algorithm was evaluated by comparing θ_{alg} with the robot orientation angle θ_{rob}. The error, ϵ_θ, was determined as follows:

$$\epsilon_\theta = |\theta_{alg} - \theta_{rob}| \quad \text{(Eq. 6)}$$

[0100] The accuracy test was repeated with a chicken tissue phantom, and the accuracy was again determined using Equations 5 and 6. For the agar phantoms, five groups of tests were performed to evaluate the algorithm execution time and accuracy. Each group consisted of seven insertions; i.e., insertion at 0, +5, +10, +15, −5, −10 and −15 degrees. The mean error as a function of insertion angle, ϵ_θ, was calculated as follows:

$$\varepsilon_\theta = \frac{\sum_{i=1}^{5} |(\theta_{alg})_i - (\theta_{rob})_i|}{5} \quad \text{(Eq. 7)}$$

Results and Conclusion

[0101] The following table presents the evaluation results. In the chicken tissue phantom, the average execution time was 0.13±0.01 seconds, and the average angulation error was 0.54±0.16 degrees. In agar phantoms, the average execution time was 0.12±0.01 seconds, and the average angulation error was 0.58±0.36 degrees. The results shown below also demonstrate that the insertion error does not significantly depend on insertion angle.

		Angle (degrees)					
		−15	−10	−5	+5	+10	+15
1	Time (seconds)	0.13	0.11	0.12	0.12	0.12	0.14
	Accuracy (degrees)	0.50	0.51	0.43	0.37	0.74	0.74
2	Time (seconds)	0.12	0.12	0.12	0.11	0.12	0.13
	Accuracy (degrees	0.30	0.71	0.48	0.68	0.42	0.86

[0102] In 3D US images, needle voxels generally have high greyscale-level values. However, due to specular reflection, some background structures may also appear to have high greyscale-level values. This increases the difficulty in automatic needle segmentation in a US image using greyscale-level information directly. As US images suffer from low contrast, signal loss due to shadowing, refraction and reverberation artifacts, the greyscale-level change detection technique of the disclosed embodiment of the invention appears to be quite robust. In addition, since the needle is segmented from a difference map, complex backgrounds can be ignored to simplify calculations and accuracy.

[0103] In conclusion, a greyscale-level change detection technique has been developed and its feasibility has been tested for near real-time oblique needle segmentation to be used in 3D US-guided and robot-aided prostate brachytherapy. The results show that the segmentation method works well in agar and chicken tissue phantoms. In addition, the approach has also been tested during several prostate cryotherapy procedures with positive results.

Alternative Methods of Defining the Region of Interest and Scan Strategies

[0104] A number of alternative methods for defining the region of interest and scan strategies have been explored for use with the system **20**. In a first alternative, the region of interest is defined to include only a set length of the needle from the tip plus a pre-determined distance beyond the needle tip along the needle trajectory. For example, the region of interest can be defined to include a one-half-inch length of the needle measured from its tip and an area one-half inch along its trajectory beyond the needle tip. The scan strategy then is selected to capture 2D US images at one-half degree intervals along the angular width of the segment of the operational scan range of the transducer of the ultrasound imaging system encompassing the region of interest. As the needle is further inserted into the target volume, the region of interest roams with the needle tip. Using this approach, 2D US images can be rapidly captured and updated to provide accurate information about the position of the needle tip.

[0105] In another alternative method for defining the region of interest and scan strategy, the region of interest is defined to include an area of expected activity of a one-half-inch length of the needle measured from its tip and an area one-half inch along its trajectory beyond the needle tip. This area of expected activity generally allows the new position of the needle to be determined when compared to previous images. A scan strategy can then be selected to scan a segment of the operational scan range of the transducer of the ultrasound

imaging system encompassing the region of interest using a fine scan density, and other areas using a coarse scan density. By selecting a relatively high scan density for the subset of the operational scan range of the transducer of the ultrasound imaging system and a relatively low scan density for other scan areas (e.g. one 2D US image every one-half degree interval in the region of interest, and every one-and-one-half degree interval outside the region of interest), detailed information about the region of interest can be obtained while still capturing a desired minimum level of detail about other areas.

[0106] Where the needle has yet to be detected, and information regarding the expected needle entry point is available, the region of interest can be defined to include an area surrounding the expected needle entry point.

[0107] Where the needle is not determined to be present in the region of interest, additional 2D images can be acquired to locate the needle.

[0108] Other alternative methods for defining the region of interest and scan strategy and combinations thereof will occur to those skilled in the art.

[0109] While the method of registering the position of an object moving in a target volume in an ultrasound imaging system and the method of imaging using an ultrasound imaging system have been described with specificity to a rotational US scanning method, other types of scanning methods will occur to those of skill in the art. For example, the same approach can be used with a linear US scanning method. In addition, the segmentation method can be applied equally well to 3D US images reconstructed using the linear scanning geometry, but acquired using rotational 3D scanning geometry such as that used in prostate imaging.

[0110] The linear regression analysis approach for determining the needle trajectory from the difference map was selected as it requires relatively low processing power. A person of skill in the art, however, will appreciate that any method of determining the needle trajectory given the difference map can be used. For example, the well-known Hough Transform technique can be employed. The Hough Transform technique requires higher computational power than the linear regression approach, but this can be ignored where such processing power is available.

[0111] While a specific method of determining the GLC threshold was disclosed, other methods of determining the GLC threshold will occur to those skilled in the art. For example, a histogram of the greyscale-level values in the 3D US image can be generated and then analyzed to determine the regions of the histogram that most likely correspond to the background and to the needle. The analysis can be based on the statistical distribution of the greyscale-level values due to the acoustic scattering of the tissue and the statistical distribution of the specular reflection of the needle.

[0112] In addition to 3D applications, difference maps can be used to register movement in a single 2D plane. In this case, the difference map could represent a 2D plane and register differences between two 2D images.

[0113] While, in the above-described embodiment, the expected needle position from the positioning software was used to determine the region of interest thereby to modify the scanning behavior of the TRUS transducer **24**, one or more previous images could be used to estimate the expected needle position. For example, where only the immediately previous image is available, the region of interest could include the needle plus a relatively large distance along its trajectory beyond the needle tip. Where two previous images are available, the region of interest could include the needle plus a distance along its trajectory beyond the needle tip, wherein the distance is determined from movement of the needle registered from the two previous images.

[0114] While, in the described embodiment, an object of interest in the ultrasound images is a needle, those skilled in the art will appreciate that the invention can be used in conjunction with other objects, such as, for example, biopsy apparatus.

[0115] It can be advantageous in some cases to compare a US image to one or more previous US images. For example, where the target volume is expected to shift, the initial image of the target volume prior to insertion of the needle may provide an inaccurate baseline image. By using more recent previous images, the target volume can be, in some cases, more readily filtered out to generate a cleaner difference map.

[0116] While the US images are pre-filtered to identify voxels that are adjacent other voxels along the expected direction that the needle longitudinally extends, other methods of filtering the images will occur to those skilled in the art. Voxels corresponding to other characteristics of an object can be identified to filter out other voxels that do not correspond to the same.

[0117] The above-described embodiments are intended to be examples of the present invention and alterations and modifications may be effected thereto, by those of skill in the art, without departing from the scope of the invention which is defined solely by the claims appended hereto.

1-31. (canceled)

32. A method of registering a needle in a patient target volume in an ultrasound imaging system, comprising:

capturing a first ultrasound image of the patient target volume using an ultrasound probe prior to insertion of the needle into said patient target volume;

capturing a second ultrasound image of a sub-sector of said patient target volume using the ultrasound probe after insertion of the needle into said patient target volume, said sub-sector corresponding generally to a predicted trajectory of the needle within said patient target volume;

computing the actual trajectory of said needle in said patient target volume using a computing device, based on differences detected between said first and second ultrasound images; and

with the actual needle trajectory computed, computing at least one of a needle tip location and an entry location of the needle into said patient target volume.

33. The method of claim **32** comprising computing both the needle tip location and the needle entry location.

34. The method of claim **33** wherein said actual needle trajectory computing comprises:

generating a difference map from said first and second ultrasound images; and

examining said difference map to determine voxels representing the needle.

35. The method of claim **34** wherein said difference map generating comprises:

comparing each pair of corresponding voxels of said first and second ultrasound images to determine a resultant difference voxel for each pair;

examining each difference voxel to determine if its magnitude exceeds a threshold; and

populating the difference map with difference voxels having magnitudes exceeding the threshold.

36. The method of claim **35** further comprising filtering the difference map to remove voxels deemed to be noise,

37. The method of claim 36 wherein said filtering comprises:
examining voxels of said difference map to detect voxels that are more than a threshold distance from the predicted needle trajectory; and
removing the detected voxels from said difference map.
38. The method of claim 37 wherein said actual needle trajectory computing further comprises:
fitting a line to the voxels in said difference map; and
using the equation of the line to represent said actual needle trajectory.
39. The method of claim 38 wherein said line is fitted to the voxels using linear regression analysis.
40. The method of claim 38 wherein said actual needle trajectory computing further comprises removing voxels in said difference map that are beyond a threshold distance from the predicted needle trajectory.
41. The method of claim 40 wherein said needle tip location computing comprises determining the voxel in said difference map that is positioned furthest along said actual needle trajectory.
42. The method of claim 41 wherein said needle entry location computing comprises calculating the intersection of the actual needle trajectory with a known needle patient target volume entry plane.
43. The method of claim 42 further comprising generating an ultrasound image of a plane within said patient target volume including said needle.
44. The method of claim 43 wherein said ultrasound image generating comprises:
capturing a third ultrasound image of the patient target volume using the ultrasound probe;
selecting an arbitrary point in said third ultrasound image;
defining a plane coplanar with the needle using the needle tip location, the needle entry location and the arbitrary point; and
extracting ultrasound image data along said plane to generate the ultrasound image of said plane.
45. The method of claim 44 wherein selecting the arbitrary point to be on a line intersecting the needle entry location and parallel to a y-axis, defines a sagital-oblique plane and wherein selecting the arbitrary point to be on a line intersecting the needle entry location and parallel to an x-axis defines a coronal oblique plane.
46. The method of claim 34 wherein said actual needle trajectory computing further comprises:
fitting a line to the voxels in said difference map; and
using the equation of the line to represent said actual needle trajectory.
47. The method of claim 46 wherein said line is fitted to the voxels using linear regression analysis.
48. The method of claim 47 wherein said actual needle trajectory computing further comprises removing voxels in said difference map that are beyond a threshold distance from the predicted needle trajectory.
49. The method of claim 48 wherein said needle tip location computing comprises determining the voxel in said difference map that is positioned furthest along said actual needle trajectory.
50. The method of claim 49 wherein said needle entry location computing comprises calculating the intersection of the actual needle trajectory with a known needle patient target volume entry plane.
51. The method of claim 50 further comprising generating an ultrasound image of a plane within said patient target volume including said needle.
52. The method of claim 51 wherein said ultrasound image generating comprises:
capturing a third ultrasound image of the patient target volume using the ultrasound probe;
selecting an arbitrary point in said third ultrasound image;
defining a plane coplanar with the needle using the needle tip location, the needle entry location and the arbitrary point; and
extracting ultrasound image data along said plane to generate the ultrasound image of said plane.
53. The method of claim 52 wherein selecting the arbitrary point to be on a line intersecting the needle entry location and parallel to a y-axis, defines a sagital-oblique plane and wherein selecting the arbitrary point to be on a line intersecting the needle entry location and parallel to an x-axis defines a coronal oblique plane.
54. A method, comprising:
imaging a patient target volume using an elongate ultraound probe and generating a three-dimensional ultrasound image of said patient target volume;
inserting a needle into said patient target volume using a needle driving apparatus;
imaging a sub-sector of said patient target volume using said elongate ultraound probe and generating a three-dimensional ultrasound image of said patient target volume sub-sector, said patient target volume sub-sector encompassing a predicted trajectory of the needle within said patient target volume;
computing the actual trajectory of said needle in said patient target volume using a computing device based on differences detected between the patient target volume three-dimensional ultrasound image and the patient target volume sub-sector three-dimensional ultrasound image; and
with the actual needle trajectory computed. computing a needle tip location and an entry location of the needle into said patient target volume.
55. The method of claim 54 further comprising:
mapping a coordinate system of said elongate ultrasound probe to a coordinate system of said needle driving apparatus; and
using needle position information from said needle driving apparatus to determine said predicted needle trajectory.
56. The method of claim 55 wherein said actual needle trajectory computing comprises:
generating a difference map from said patient target volume and patient target volume sub-sector ultrasound images; and
examining said difference map to determine voxels representing the needle.
57. The method of claim 56 wherein said difference map generating comprises:
comparing each pair of corresponding voxels of said patient target volume and patient target volume sub-sector ultrasound images to determine a resultant difference voxel for each pair;
examining each difference voxel to determine if its magnitude exceeds a threshold; and
populating the difference map with difference voxels having magnitudes exceeding the threshold.

58. The method of claim **57** further comprising filtering the difference map to remove voxels deemed to be noise.

59. The method of claim **58** wherein said filtering comprises:

examining voxels of said difference map to detect voxels that are more than a threshold distance from the predicted needle trajectory; and

removing the detected voxels from said difference map.

60. The method of claim **59** wherein said actual needle trajectory computing further comprises:

fitting a line to the voxels in said difference map; and

using the equation of the line to represent said actual needle trajectory.

61. The method of claim **60** wherein said line is fitted to the voxels using linear regression analysis.

62. The method of claim **60** wherein said actual needle trajectory computing further comprises removing voxels in said difference map that are beyond a threshold distance from the predicted needle trajectory.

63. The method of claim **62** wherein said needle tip location computing comprises determining the voxel in said difference map that is positioned furthest along said actual needle trajectory.

64. The method of claim **63** wherein said needle entry location computing comprises calculating the intersection of the actual needle trajectory with a known needle patient target volume entry plane.

65. The method of claim **63** further comprising generating an ultrasound image of a plane within said patient target volume including said needle.

66. The method of claim **65** wherein said ultrasound image generating comprises:

capturing a third ultrasound image of the patient target volume using said elongate ultrasound probe;

selecting an arbitrary point in said third ultrasound image;

defining a plane coplanar with the needle using the needle tip location, the needle entry location and the arbitrary point; and

extracting ultrasound image data along said plane to generate an ultrasound image of said plane.

67. The method of claim **60** further comprising generating an ultrasound image of a plane within said patient target volume including said needle.

68. The method of claim **67** wherein said ultrasound image generating comprises:

capturing a third ultrasound image of the patient target volume using said elongate ultrasound probe;

selecting an arbitrary point in said third ultrasound image;

defining a plane coplanar with the needle using the needle tip location, the needle entry location and the arbitrary point; and

extracting ultrasound image data along said plane to generate an ultrasound image of said plane.

69. A system, comprising:

an ultrasound transducer imaging a patient target volume prior to insertion of a needle in said patient target volume and imaging a sub-sector of said patient target volume after insertion of the needle in said patient target volume, said patient target volume sub-sector encompassing a predicted trajectory of the needle within said patient target volume;

a needle driving apparatus for inserting a needle into said patient target volume; and

a processor communicating with said ultrasound transducer and said needle driving apparatus, said processor computing the actual trajectory of said needle in said patient target volume using differences detected between the imaged patient target volume and the imaged patient target volume sub-sector and with the actual needle trajectory computed, said processor computing a needle tip location and an entry location of the needle into said patient target volume.

70. The system of claim **69** wherein said processor maps a coordinate system of said ultrasound transducer to a coordinate system of said needle driving apparatus and uses needle position information from said needle driving apparatus to determine said predicted needle trajectory.

71. The system of claim **70** wherein during actual needle trajectory computing, said processor generates a difference map from said imaged patient target volume and said imaged patient target volume sub-sector and examines said difference map to determine voxels representing the needle.

72. The system of claim **71** wherein during difference map generating, said processor compares each pair of corresponding voxels of said imaged patient target volume and said imaged patient target volume sub-sector to determine a resultant difference voxel for each pair, examines each difference voxel to determine if its magnitude exceeds a threshold and populates the difference map with difference voxels having magnitudes exceeding the threshold,

73. The system of claim **72** wherein said processor filters the difference map to remove voxels deemed to be noise.

74. The system of claim **71** wherein during actual needle trajectory computing, said processor fits a line to the voxels in said difference map and uses the equation of the line to represent said actual needle trajectory.

75. The system of claim **74** wherein during needle tip location computing, said processor determines the voxel in said difference map that is positioned furthest along said actual needle trajectory.

76. The method of claim **75** wherein during needle entry location computing, said processor calculates the intersection of the actual needle trajectory with a known needle patient target volume entry plane.

77. The method of claim **74** wherein said processor generates an ultrasound image of a plane within said patient target volume including said needle.

78. The method of claim **77** wherein during ultrasound image generating, said processor captures a third ultrasound image of the patient target volume, selects an arbitrary point in said third ultrasound image, defines a plane coplanar with the needle using the needle tip location, the needle entry location and the arbitrary point and extracts ultrasound image data along said plane to generate an ultrasound image of said plane.

* * * * *

专利名称(译)	超声成像系统和使用其的成像方法		
公开(公告)号	US20120004539A1	公开(公告)日	2012-01-05
申请号	US13/233449	申请日	2011-09-15
申请(专利权)人(译)	罗伯兹研究所		
当前申请(专利权)人(译)	罗伯兹研究所		
[标]发明人	GARDI LORI ANNE DOWNEY DONAL B FENSTER AARON		
发明人	GARDI, LORI ANNE DOWNEY, DONAL B. FENSTER, AARON		
IPC分类号	A61B8/00 A61B8/08 G06T7/20		
CPC分类号	A61B8/0833 A61B10/0233 A61B19/2203 A61B2019/5276 A61B8/483 G06T7/004 G06T7/2053 G06T2207/30004 A61B2019/5289 G06T7/70 A61B34/30 A61B2090/364 A61B2090/378 G06T7/254		
优先权	11/585984 2007-07-18 US 60/535825 2004-01-13 US PCT/CA2005/000032 2005-01-12 WO		
其他公开文献	US9070190		
外部链接	Espacenet USPTO		

摘要(译)

在超声成像系统中记录在目标体积中移动的对象的位置的方法包括捕获目标体积的第一超声图像。然后在捕获第一超声图像之后捕获目标体积的第二超声图像。使用在第一和第二超声图像之间检测到的差异来识别目标体积中的对象的位置。在另一方面，确定目标体积中的感兴趣区域。确定包含感兴趣区域的超声成像系统的换能器的操作扫描范围的片段。在图像捕获期间，换能器聚焦在操作扫描范围的区段上。